Heliyon 10 (2024) e35491

Contents lists available at ScienceDirect

Heliyon

journal homepage: www.cell.com/heliyon

Research article

# Mechanism investigation of anti-NAFLD of Shugan Yipi Granule based on network pharmacology analysis and experimental verification

Hairong Li [a,b,c], lijun Niu [d], Meiling Wang [e], Chunmei Liu [e], Yunlong Wang [f], Yu Su [e], Yubin Yang [a,b,*]

[a] West China Second University Hospital, Sichuan University, Chengdu, 610000, China
[b] Key Laboratory of Birth Defects and Related Diseases of Women and Children (Sichuan University), Ministry of Education, China
[c] Guangdong Pharmaceutical University, Xiaoguwei street, Panyu District, Guangzhou, 510006, China
[d] Department of Anesthesiology, The First Affiliated Hospital of Sun Yat-sen University, Guangzhou, 510080, China
[e] The First Affiliated Hospital of Guangdong Pharmaceutical University, Nonglin Xia Road, Yuexiu District, Guangzhou, 510006, China
[f] Academic Department, Giant Praise (HK) Pharmaceutical Group Limited, Changchun, 130033, China

ARTICLE INFO

*Keywords:*
Shugan yipi granule
NAFLD
Non-targeted metabolomics
Network pharmacology
In-vitro experiments

ABSTRACT

As a classical traditional Chinese patent medicine, Shugan Yipi Granule is widely used in China to treat non-alcoholic fatty liver disease (NAFLD) recently. Our previous study confirmed that Shugan Yipi Granule are effective in NAFLD. However, its underlying mechanism is still unknown. This study aims to investigate the mechanism of Shugan Yipi Granule on NAFLD based on network pharmacology prediction, liquid chromatography-mass spectrometry (LC-MS) analysis and in vitro verification. We obtained the active ingredients and targets of Shugan Yipi Granule and NAFLD from 6 traditional Chinese medicine databases, and the crucial components and targets screened by protein-protein interaction (PPI) network were used for molecular docking. Plasma metabolomics of NAFLD patients treated with Shugan Yipi Granule for one month was analyzed using LC-MS methods and MetaboAnalyst 4.0 to obtain significant differential metabolites and pathways. Finally, free fatty acid (FFA) induced HepG2 cells were treated with different concentrations of quercetin and kaempferol, then oil red o (ORO) and triglyceride (TG) level were tested to verify the lipid deposition of the cell. Network pharmacology analysis showed that the main active ingredients of Shugan Yipi Granule include quercetin, kaempferol and other 58 ones, as well as 188 potential targets. PI3K/Akt signaling pathway was found to be the most relevant pathway for the treatment of NAFLD. Non-targeted metabolomics showed that quercetin and kaempferol were significantly up-regulated differential metabolites and were involved in metabolic pathways such as thyroid hormone signaling. In vitro results showed that quercetin, kaempferol were effective in reducing lipid deposition and TG content by inhibiting cellular fatty acid uptake. Ultimately, with the network pharmacology and serum metabolomics analysis, quercetin and kaempferol were found to be the important active ingredients and significantly up-regulated differential metabolites of Shugan Yipi Granule against NAFLD, which we inferred that they may regulate NAFLD through PI3K/Akt signaling pathway and thyroid hormone metabolism pathway. The in vitro experiment verification results showed that quercetin and kaempferol attenuated the lipid accumulation and TG content by inhibiting the fatty acid uptake in the FFA-

* Corresponding author. West China Second University Hospital, Sichuan University, Chengdu, 610000, China.
*E-mail address:* myxs32@126.com (Y. Yang).

https://doi.org/10.1016/j.heliyon.2024.e35491
Received 7 May 2024; Received in revised form 24 July 2024; Accepted 30 July 2024
Available online 5 August 2024

induced HepG2 cell. Current study provides the necessary experimental basis for subsequent in-depth mechanism research.

## 1. Introduction

Currently, the incidence of NAFLD in Asia is approximately 24.7 %, while the global prevalence has reached 25 %, and nearly 80 million people are affected in the United States alone [1]. Most recent evidence highlights NAFLD is a much more complex disease [2]. Its manifestations include a variety of clinical phenotypes, ranging from simple steatosis NAFLD to non-alcoholic steatohepatitis (NASH), non-inflammatory fibrosis and cirrhosis [2]. In view of the number of affected individuals and these complex complications, it severely reduced the quality of life and well-being of people and will impose significant health and economic burden on patients, families as well as society [3].

Traditional Chinese Medicine (TCM) plays a significant role in treating NAFLD in Asian countries [4,5]. TCM is an indispensable source for exploring the treatment of liver diseases [6]. Shugan Yipi Granule is a classic traditional Chinese prescription for treating acute and chronic hepatitis, with the effect of clearing heat and preventing dampness syndrome [7]. It has also achieved great therapeutic effects in treating NAFLD with dampness and heat syndrome [8]. Shugan Yipi Granule has the function of clearing dampness and heat, soothing the liver, and alleviating the gallbladder. It comprises 6 herbs: *Artemisiae scopariae herba* (Yinchen), *Astragali radix* (Huangqi), *Crataegi fructus* (Shanzha), *Schisandrae chinensis fructus* (Wuweizi), *Poria* (Fuling), *Taraxaci herba* (Pugongying). Flavones of Astragalus (Huangqi), including β-sitosterol, formononetin, calycosin and glucoside, could improve insulin resistance and inflammation [9], ameliorate liver fibrosis [10] and prevent NASH as well [4]. Vitexin, a compound of Crataegi fructus (Shanzha), has the effect of ameliorating the chronic stress response of NAFLD mice induced by high fat diet (HFD) through inhibition of TLR4/NF-kappa B signaling pathway and regulating the expression of proteins like fatty acid synthase (FAS) and sterol regulatory element-binding protein 2(SREBP2) that associated with fatty acid synthesis [11]. Taraxacum leaf extracts like caffeic acid, chlorogenic acid and luteolin significantly inhibited lipid accumulation in the livers of high fat diet (HFD)-fed C57BL6J mice via activation of AMPK signaling pathway, as well as improve glucose disposal in insulin-resistant mice [12].

However, up to date, there are few mechanisms analysis of Shugan Yipi Granule on NAFLD, and its possible mechanism is still unclear. Network pharmacology is a holistic analysis strategy that can reveal the mechanism of traditional Chinese prescriptions, systematically analyze the interaction network between active ingredients, key targets, and crucial pathways, and effectively create a Drug-component-target-pathway-disease (D-C-T-P-D) network to reveal the overall mechanism of drug action on diseases [13]. Metabolomics is the study of small molecule metabolites in organisms, which reflects the overall metabolic, physiological and pathological state of the organism by determining the dynamic changes of metabolites in the body. Its overall research strategy based on endogenous metabolites is consistent with the "multi-component, multi-objective, and overall regulation" of traditional Chinese prescriptions [14]. In addition, further validation of the main active ingredients of Shugan Yipi Granule on NAFLD was conducted

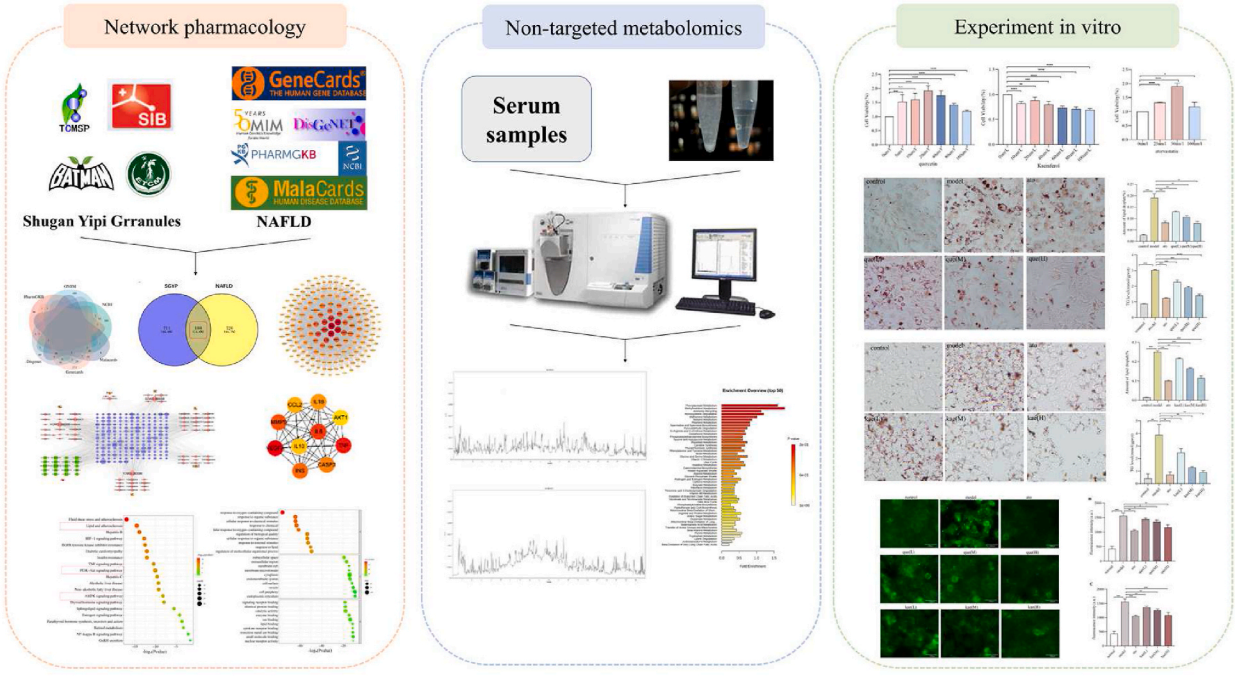


**Fig. 1.** Flowchart of current study.

through in vitro experiments. We induced HepG2 cells with free fatty acids to construct in vitro NAFLD model, ORO and TG levels were assayed to evaluate the effect of quercetin and kaempferol on lipid deposition, then the fatty acid uptake capacity of the HepG2 cell were detected by fluorescence method.

Therefore, by combining network pharmacology, molecular docking, non-targeted metabolomics and in vitro experiment, we can study the effect and mechanism of traditional Chinese prescriptions and predict the material basis of its efficacy. Current study ultimately provides preliminary network and metabolomics prediction reference results for the pharmacological research of Shugan Yipi Granule in the future therapy of NAFLD. The flowchart of this study is shown in Fig. 1.

## 2. Materials and methods

### 2.1. Network pharmacology analysis

#### 2.1.1. Identification of active components and targets of Shugan Yipi Granule

The ingredients of Shugan Yipi Granule were screened from TCMSP (https://old.tcmsp-e.com/tcmsp.php) [15], BATMAN-TCM (http://bionet.ncpsb.org.cn/batman-tcm/) [16] and ETCM database (http://www.tcmip.cn/ETCM/index.php/Home/Index/) [17]. According to the characteristics of pharmacokinetics absorption distribution metabolism and excretion (ADME), the final chemical compounds were screened out by the screening threshold of the oral bioavailability (OB) value $\geq$ 30 % and the drug-like properties (DL) value $\geq$ 0.18 % [18]. Targets of Shugan Yipi Granule were retrived from following databases, namely TCMSP, BATMEN-TCM, ETCM and SwissTargetPrediction (http://www.swisstargetprediction.ch/) [19]. Shugan Yipi Granule-related targets were finally gained by integrating the results from previous mentioned 4 databases and removing redundant.

#### 2.1.2. Disease targets screening

Targets of NAFLD were screened from 6 databases: GeneCards (http://www.genecards.org/) [20], OMIM (http://omim.org/) [21], PharmGKB (http://www.pharmgkb.org/) [22], DisGeNET (http://www.gisgenet.org/home) [23], DrugBank (http://www.drugbank.ca/) [24] and NCBI (https://www.ncbi.nlm.nih.gov/) [25]. NAFLD-related targets were finally established by gathering the search results from above 6 databases and deleting redundant. Ultimately, all targets were converted into standard gene names through UniProt (https://www.unipr ot. org/) platform [26]. Finally, the potential targets of Shugan Yipi Granule act on NAFLD were obtained by using Venn diagram online tool (http://bioinfo.cnb.csic.es/tools/venny/index.html).

#### 2.1.3. Construction of protein-protein interaction (PPI) network and selection of core targets

In order to screen out the significant targets and to analyze interactions between proteins, these potential targets were imported into the STRING database (https://string-db.org) [27] with the condition of choosing "*Homo sapiens*" at the interface to construct the PPI network. The minimum required interaction score was "high confidence (0.7)" and disconnected nodes were hidden in the network [28], then the PPI network was constructed. Subsequently, the PPI network was saved in "tsv" file format, which was imported into Cytoscape 3.9.1 software (https://www.cytoscape.org/), to analyze the results by the network topology analysis function. In the PPI network, we ranked the targets according to the degree value. Further network interaction analysis of common targets was performed using network plug-ins [29]. Top 10 hub genes were retrieved by using the CytoHubba [30], these hub genes have the highest degree of connectivity and maximal clustering centrality [31]. Then, the target sub-networks were identified from the PPI network by using the MCODE plugin.

#### 2.1.4. Gene ontology (GO) and kyoto encyclopedia of genes and genomes (KEGG) enrichment analysis and drug-components-targets-pathways-disease (D-C-T-P-D) network

The underlying targets of Shugan Yipi Granule in the treatment of NAFLD were imported into g:Profiler database (https://biit.cs.ut.ee/gprofiler/gost) [32] to collect GO and KEGG analysis. GO analysis is used to screen biological processes (BP), cellular components (CC) and molecular functions (MF) [33]. KEGG enrichment analysis can find important signaling pathways involved in biological processes. Subsequently, top 20 highly enriched pathways as well as the top 10 highly enriched GO terms were sorted into a table and then uploaded into bioinformatics (https://www.bioinformatics.com.cn/) [34] to obtain bubble diagram of enrichment analysis. Shugan Yipi Granule, 6 herbal medicines, main active compounds, 188 key targets, significant pathways and NAFLD were imported into Cytoscape (version 3.9.1) platform to establish a D-C-T-P-D network, which systematically analyzed the interaction among them. The topological parameters, degrees and betweenness centrality (BC) of each node were calculated and the main active components, key targets as well as significant pathways were screened out.

#### 2.1.5. Molecular docking

According to the D-C-T-P-D network analysis, main active compounds highly related to the hub genes were selected as ligands, hub genes were chosen as the receptor proteins for molecular docking [35]. The detailed steps are as follows: First, the 3D "sdf" file of compounds from Pubchem database (https://pubchem.ncbi.nlm.nih.gov) were downloaded and converted into mol2 format through OpenBabel-3.1.1 software, the PDB file of 3D structures for proteins were collected from the PDB website (https://www.rcsb.org) [36]. Then, PyMOL (https://pymol.org/2/) [37] software was utilized to delete water molecules and needless ligands [38], the receptor proteins were hydrogenated and charge calculated through the AutoDockTools-1.5.7 (https://autodock.scripps.edu/) [39] and outputted as "pdbqt" files. Hereafter, the prepared "pdbqt" files of the receptors and ligands were imported into AutoDockTools-1.5.7 for molecular docking. Before running the auto dock grid, ensure the grid boxes covering the entire protein to facilitate blind docking

[35]. The auto dock between the active compounds and receptor proteins then was conducted in AutoDockTools-1.5.7 to evaluate the free binding affinity. A lower binding energy indicates a higher affinity and a more stable conformation between receptors and ligands [40]. Eventually, the lowest binding data were collected and visualized through the PyMOL software.

### 2.2. Non-targeted metabolomics

#### 2.2.1. Ethics statement

The clinical study of Shugan Yipi Granule (Plasma metabolomics) has been approved by the Clinical Research Ethics Committee of the First Affiliated Hospital of Guangdong Pharmaceutical University. Signed informed consent was obtained from all participants.

#### 2.2.2. Study participants and research design

6 patients with NAFLD were given Shugan Yipi Granule produced by Yuanhesheng (Jilin) Pharmaceutical Co., LTD. After administered 10 g three times a day for one month, serum samples were collected from the patients in fasting state for non-targeted metabolomics analysis.

#### 2.2.3. Instruments and reagents

Ultra High Performance Liquid Chromatography (UHPLC) (Agilent 1290, Agilent Technologies), High Resolution Mass Spectrometry (HRMS) (Agilent 6545 QTOF, Agilent Technologies), Acetonitrile (Merck: Darmstadt, Germany), Methanol (Merck: Darmstadt, Germany), Formic acid (CNW: Shanghai, China), ammonium acetate (CNW: Shanghai, China), Ultrapure water (Merck: (Darmstadt, Germany).

#### 2.2.4. Serum sample pretreatment

800μl methanol acetonitrile is added into the 200ul serum sample, then vortex for 30s, ultrasonic for 10min (4 °C water bath), placed in −20 °C environment for 60min, centrifuge at 13000 rmp for 15min. 800ul of supernatant was placed in a 35 °C vacuum environment for drainage, and then the sample was dissolved in 300ul of 50 % acetonitrile solution. The sample then was vortexed for 30 s, sonicated for 10 min, and centrifuged at 4 °C at 13000 rpm. Finally, 150ul of supernatant was taken for computer analysis.

#### 2.2.5. Chromatographic and mass spectrometric conditions

Control the column temperature at 35 °C and sample volume at 1 μL. Mobile phase A in positive ionization mode was consisted of 1000:1 ratio of water and formic acid; mobile phase B was consisted of 1000:1 ratio of acetonitrile and formic acid. Mobile phase A in negative ionization mode is water and 2 mm $CH_3COONH_4$, and mobile phase B is acetonitrile. The Agilent 6545A QTOF mass spectrometer was controlled by the control software (LC/MS data acquisition, version B.08.00) for primary and secondary mass spectrometry data acquisition in automatic MS/MS mode with a mass scan range of $m/z$ (50–1100). Positive and negative ion modes were used to collect data.

#### 2.2.6. Statistical analysis

Analysis Base File Converter is used to convert data into ABF format. MSDIAL3.08 software is used to process data such as peak finding and peak correction of ABF files, and retrieve according to the main and auxiliary graphs. The identification results were obtained by integrating Metlin, MassBank, MoNA and HMDB databases (version 2.0). For the identification data of MSDIAL alignment, statistical analysis was performed only by controlling Quality Control (QC) sample index CV to be less than 30 %. Finally, the Total Ion Chromatography (TIC) ion summation was normalized and the MetaboAnalyst 4.0 software was used for difference and enrichment analysis.

### 2.3. In vitro experimental validation

#### 2.3.1. Chemicals and reagents

Quercetin (Apex BIO Biotechnology Co., Ltd. in the United States, lot No. N1841-1000); Atorvastatin (Apex BIO Biotechnology Co., Ltd. in the United States, lot No. C6405-50); Kaempferol (Apex BIO Biotechnology Co., Ltd. in the United States, No. N1719-50); Palmitic acid (Apex BIO Biotechnology Co., Ltd. in the United States, lot No. N2456-5000); Oleic acid (Apex BIO Biotechnology Co., Ltd. in the United States, lot No. C4977-1000); Saturated oil red o Dyeing Solution (Wuhan Saiweier Biotechnology Co., Ltd, lot No. G1015-100 ML); DMEM (Wuhan Saiweier Biotechnology Co., Ltd, lot No. G4511-500 ML); Penicillin mixture (Wuhan Saiweier Biotechnology Co., Ltd, lot No. G4003-100 ML); Bovine Serum Albumin(Wuhan Saiweier Biotechnology Co., Ltd, lot No. GC305010-25 g); Fetal bovine serum (Wuhan Saiweier Biotechnology Co., Ltd, lot No. G8002-100 ML); 0.25 % trypsin digestion solution (Wuhan Saiweier Biotechnology Co., Ltd, lot No. G4001-100 ML); Triglyceride (TG) determination kit (Nanjing Jiancheng Biotechnology Research Institute Co., Ltd, lot No. A110-2-1); Fatty Acid Uptake Assay Kit (Tohren Chemical Technology (Shanghai) Co. No. UP07-100tests)

#### 2.3.2. Solution preparation

The preparation of free fatty acid (FFA): The preheated dissolved 20 mmol/L oleic acid (OA) solution and palmitic acid (PA) solution were added into 30 % BSA solution, and coupled in a water bath at 37 °C for 1 h to obtain the OA-BSA solution and PA-BSA solution with a concentration of 10 mM; OA-BSA solution and PA-BSA solution were added according to the ratio of OA:PA = 2:1,

**Table 1**
Detail information of 60 ingredients.

| Mol ID | Molecule name | oral bioavailability (OB)% | drug-like properties (DL) |
|---|---|---|---|
| MOL000289 | pachymic acid | 33.63 | 0.81 |
| MOL008045 | 4′-Methylcapillarisin | 72.18 | 0.35 |
| MOL008041 | Eupatolitin | 42.55 | 0.37 |
| MOL008040 | Eupalitin | 46.11 | 0.33 |
| MOL008039 | Isoarcapillin | 57.40 | 0.41 |
| MOL007274 | Skrofulein | 30.35 | 0.30 |
| MOL005573 | Genkwanin | 37.13 | 0.24 |
| MOL004609 | Areapillin | 48.96 | 0.41 |
| MOL000098 | quercetin | 46.43 | 0.28 |
| MOL000239 | Jaranol | 50.83 | 0.29 |
| MOL000354 | isorhamnetin | 49.6 | 0.31 |
| MOL000371 | 3,9-di-O-methylnissolin | 53.74 | 0.48 |
| MOL000380 | (6aR,11aR)-9,10-dimethoxy-6a,11a-dihydro-6H-benzofurano[3,2-c]chromen-3-ol | 64.26 | 0.42 |
| MOL010586 | formononetin | 66.39 | 0.21 |
| MOL000417 | Calycosin | 47.75 | 0.24 |
| MOL000422 | kaempferol | 41.88 | 0.24 |
| MOL004624 | Longikaurin A | 47.72 | 0.53 |
| MOL008968 | Gomisin-A | 30.69 | 0.78 |
| MOL000273 | (2R)-2-[(3S,5R,10S,13R,14R,16R,17R)-3,16-dihydroxy-4,4,10,13,14-pentamethyl-2,3,5,6,12,15,16,17-octahydro-1H-cyclopenta[a]phenanthren-17-yl]-6-methylhept-5-enoic acid | 30.93 | 0.81 |
| MOL000280 | (2R)-2-[(3S,5R,10S,13R,14R,16R,17R)-3,16-dihydroxy-4,4,10,13,14-pentamethyl-2,3,5,6,12,15,16,17-octahydro-1H-cyclopenta[a]phenanthren-17-yl]-5-isopropyl-hex-5-enoic acid | 31.07 | 0.82 |
| MOL000285 | (2R)-2-[(5R,10S,13R,14R,16R,17R)-16-hydroxy-3-keto-4,4,10,13,14-pentamethyl-1,2,5,6,12,15,16,17-octahydrocyclopenta[a]phenanthren-17-yl]-5-isopropyl-hex-5-enoic acid | 38.26 | 0.82 |
| MOL000398 | isoflavanone | 109.99 | 0.3 |
| MOL000378 | 7-O-methylisomucronulatol | 74.69 | 0.3 |
| MOL000438 | (3R)-3-(2-hydroxy-3,4-dimethoxyphenyl) chroman-7-ol | 67.67 | 0.26 |
| MOL008957 | Schizandrer B | 30.71 | 0.83 |
| MOL008974 | Gomisin G | 32.68 | 0.83 |
| MOL000296 | hederagenin | 36.91 | 0.75 |
| MOL000300 | dehydroeburicoic acid | 44.17 | 0.83 |
| MOL000291 | Poricoic Acid B | 30.52 | 0.75 |
| MOL000275 | trametenolic acid | 38.71 | 0.8 |
| MOL000290 | Poricoic acid A | 30.61 | 0.76 |
| MOL000358 | beta-sitosterol | 36.91 | 0.75 |
| MOL008047 | Artepillin A | 68.32 | 0.24 |
| MOL007719 | Deoxyshikonin | 73.85 | 0.18 |
| MOL005317 | Deoxyharringtonine | 39.27 | 0.81 |
| MOL000276 | 7,9(11)-dehydropachymic acid | 35.11 | 0.81 |
| MOL008043 | capillarisin | 57.56 | 0.31 |
| MOL008046 | Demethoxycapillarisin | 52.33 | 0.25 |
| MOL008992 | Wuweizisu C | 46.27 | 0.84 |
| MOL006554 | Taraxerol | 38.4 | 0.77 |
| MOL001645 | Linoleyl Acetate | 42.1 | 0.2 |
| MOL008956 | Angeloylgomisin O | 31.97 | 0.85 |
| MOL008978 | Gomisin R | 34.84 | 0.86 |
| MOL001979 | Lanosterol | 42.12 | 0.75 |
| MOL000279 | Cerevisterol | 37.96 | 0.77 |
| MOL000282 | ergosta-7,22E-dien-3beta-ol | 43.51 | 0.72 |
| MOL000283 | Ergosterol peroxide | 40.36 | 0.81 |
| MOL000287 | 3beta-Hydroxy-24-methylene-8-lanostene-21-oic acid | 38.7 | 0.81 |
| MOL000292 | poricoic acid C | 38.15 | 0.75 |
| MOL000033 | (3S,8S,9S,10R,13R,14S,17R)-10,13-dimethyl-17-[(2R,5S)-5-propan-2-yloctan-2-yl]-2,3,4,7,8,9,11,12,14,15,16,17-dodecahydro-1H-cyclopenta[a]phenanthren-3-ol | 36.23 | 0.78 |
| MOL000211 | Mairin | 55.38 | 0.78 |
| MOL002680 | Flavoxanthin | 60.41 | 0.56 |
| MOL004492 | Chrysanthemaxanthin | 38.72 | 0.58 |
| MOL000374 | 5′-hydroxyiso-muronulatol-2′,5′-di-O-glucoside | 41.72 | 0.69 |
| MOL000387 | Bifendate | 31.1 | 0.67 |
| MOL000439 | isomucronulatol-7,2′-di-O-glucosiole | 49.28 | 0.62 |
| MOL000433 | FA | 68.96 | 0.71 |
| MOL011455 | 20-Hexadecanoylingenol | 32.7 | 0.65 |
| MOL000442 | 1,7-Dihydroxy-3,9-dimethoxy pterocarpene | 39.05 | 0.48 |
| MOL000379 | 9,10-dimethoxypterocarpan-3-O-β-D-glucoside | 36.74 | 0.92 |

and the FFA solution was obtained as 10 mmol/L after mixing. The FFA solution was filtered through a 0.22 μm membrane for sterilization, and stored at −20 °C for spare parts. Dilute the solution with culture medium to the desired concentration.

#### 2.3.3. Cell culture and cell model establishment

After thawing and resuscitation, HepG2 cells were cultured in DMEM medium containing 10 % fetal bovine serum and 1 % double antibody, placed in an incubator at 37 °C with 5 % $CO_2$, and then routinely digested, passaged, and frozen when the cells proliferated to 75 %–85 %. The fatty acid master batch was prepared with the molar volume ratio of sodium oleate and sodium palmitate of 2:1. Dilute the fatty acid master batch with the complete medium, and dilute it to 1 mmol/$L^{-1}$ fatty acid modeling solution [41].

#### 2.3.4. Cell viability by CCK8

HepG2 cells were divided into normal group, model group, positive control group and experimental group. Cells in the normal group were cultured with complete medium; cells in the model group were cultured with 1 mmol/$L^{-1}$ fatty acid modeling solution; cells in the positive control group were cultured in 1 mmol/$L^{-1}$ fatty acid modeling solution with the addition of atorvastatin at a concentration of 50 μmol/$L^{-1}$; cells from the experimental group were incubated in 1 mmol/$L^{-1}$ fatty acid model solution followed by the addition of different concentrations of quercetin and kaempferol. The indexes of each group were detected 24 h after the intervention.

#### 2.3.5. Oil red O staining for cellular fat Degeneration

Inoculate HepG2 cells into 6-well plates, after wall attachment, discard complete medium, wash with phosphate buffer, add cell culture medium without fetal bovine serum, and synchronize cell differentiation for 12 h. Discard medium, wash with phosphate buffer, and intervene in the group according to "2.3.3" for 24 h. After 24 h, discard medium, wash with phosphate buffer, and add 4 % paraformaldehyde to fix the cells for 20–30 min. After 24 h, discard the medium, wash with phosphate buffer, fix with 4 % paraformaldehyde for 20–30 min, discard the fixative, wash with distilled water, add 60 % isopropanol for 5 min and discard, add freshly configured saturated oil red O dye solution for 15 min and discard the dye solution. Stain cells for 15 min, discard dye solution, rinse with distilled water until there is no excess dye solution, add a small amount of distilled water to cover the cells, and observe under a microscope. Oil red O dye solution can dye lipid droplets into orange-red color.

#### 2.3.6. GPO-PAP enzyme assay for TG content in each group of cells

The cell suspension was prepared 24 h after drug intervention, broken by ultrasonication in an ice bath, sampled according to the reagent instruction, mixed, incubated, and the optical density (OD) value of each group was measured at 500 nm on an enzyme labeling instrument, and the total protein concentration of the cells in each group was measured by the Bicinchoninic acid (BCA) method, to calculate the TG content.

#### 2.3.7. Detection of free fatty acid uptake

The fatty acid uptake probe in the fatty acid uptake assay kit (Tohren Chemical Technology (Shanghai) Co. No.UP07-100tests) is used as a fatty acid analogue to directly display the cell's ability to take up fatty acids [42–44]. HepG2 cells were inoculated into 6-well plates at 30,000 wells per well, cells in each group were administered for 24 h follow the steps of "2.3.3", samples were spiked according to steps of the Fatty Acid Uptake Kit, then observed and photographed by a fluorescence microscope, and the results were analyzed by measuring the wavelengths with the use of Varioskan LUX multimode microplate reader.

#### 2.3.8. Statistical analysis

The experimental results were statistically processed using GraphPad Prism-9.5 software. The analysis method of T test was used for comparison between groups. The difference with $*P < 0.05$ or $**P < 0.01$ is statistically significant. Each experiment was repeated for more than 3 times independently.

## 3. Results

### 3.1. Network pharmacology

#### 3.1.1. Targets of the Shugan Yipi Granule and NAFLD

60 candidate components of Shugan Yipi Granule were screened out, including 3 kinds of *Taraxaci herba* (Pugongying), 5 kinds of *Crataegi fructus* (Shanzha), 12 kinds of *Artemisiae scopariae herba* (Yinchen), 15 kinds of *Poria* (Fuling), 20 kinds of *Astragali radix* (Huangqi) and 9 kinds of *Schisandrae chinensis fructus* (Wuweizi). 899 potential targets for Shugan Yipi Granule were collected from the databases. Details of the 60 components are provided in Table 1. Relevant information on the putative target of the active components were displayed in Table S1. By entering the keyword "nonalcoholic fatty liver" and using the correlation score ≥4.37 [45] obtained by the twice median screening method as the screening criterion, 517 genes were retrieved from Genecards database. Score≥0.1 was used as a criterion to filter 140 related disease genes from the DisGeNET database [46]. Furthermore, there were 136, 527, 405 and 47 NAFLD genes were screened from the Malacards, OMIM, NCBI and pharmGBK database respectively. And the species was restricted to humans. Ultimately, after merging the targets of the above 6 databases and deleting redundant ones, an overall of 914 related disease genes remained for further analysis (Fig. 2A). The relevant information of disease genes is provided in Table S2.

#### 3.1.2. Construction of PPI network

188 common targets of Shugan Yipi Granule and NAFLD were obtained and then visualized by Venn diagram (Fig. 2B). These 188 targets were selected as the potential targets to evaluate the anti-NAFLD activity of Shugan Yipi Granule. Genes like FOLR2 and TNNI3K didn't interact with the other targets were removed. PPI network was established with the remaining 186 targets, including 186 nodes and 3316 edges (Fig. 2C). In this network, each node represents different targets, while the edges represent interaction relationships among the targets. In general, the larger the size of the nodes, the darker the color, the higher the degree value, and the more intimate the interaction with the other nodes is. MCODE plugin in Cytoscape was then used to cluster the PPI network. Accordingly, top 3 clusters were displayed in Fig. 2E. CytoHubba is used to calculate the degree of protein interaction. The top 10 genes were selected as hub genes following the CytoHubba network analysis (Fig. 2D). These 10 hub genes (INS, AKT, TNF, IL6, MMP9, IL1B, IL10, CCL2, CASP3, VEGFA) may be the essential targets of the Shugan Yipi Granule in treating NAFLD.

#### 3.1.3. GO, KEGG enrichment analysis and establishment of D-C-T-P-D network

Based on the $p$ value ($p \leq 0.05$) as well as the amounts of enriched targets, the top 10 enriched biological processes (BP), cellular components (CC) and molecular functions (MF) as well as the top 20 highly enriched pathways were elected for visualization, illustrated via bubble diagrams (Fig. 4). As presented in Fig. 2F, the BP include the response to lipid, the cellular response to chemical stimulus and so on, the CC included cytoplasm, endomembrane system, extracellular space, and the like, the MF involving catalytic activity, lipid binding and so on. As can be seen in Fig. 2G, the majority of the genes are involved in the following pathways: PI3K-AKT signaling pathway, AMPK signaling pathway and NF-Kappa B singling pathway. As shown in the network (Fig. 2H), purple circle nodes represent the key targets, triangle nodes represent the 6 herbs, diamond-shaped nodes with different colors represents the crucial compounds of the 6 herbs and the green square nodes represents the 20 pathways that Shugan Yipi Granule acts on NAFLD. Specifically, the compounds with the highest degree (score>30) were Quercetin (MOL000098), Pachymic acid (MOL000289), isorhamnetin (MOL000354), trametenolic acid (MOL000275) and Demethoxycapillarisin (MOL008046), manifesting that these compounds may be crucial compounds for Shugan Yipi Granule against NAFLD. Moreover, the targets with highest degree were AKT1, INS, IL10, IL6.

#### 3.1.4. Molecular docking validation

Through the analysis of D-C-T-P-D network (Fig. 2H), 5 main active compounds with the highest degree were selected as receptors, and the 10 hub genes were used as ligands. Fig. 3A1-A4 displayed the first 4 pairs of docking processes with the lowest binding energy, and the other 6 pairs of docking processes are displayed in Supplementary Fig. 2. Detailed binding energy information is shown in Fig. 3B. The lower binding energy indicates a more stable binding conformation between the receptors and ligands [47]. As can be seen in Fig. 3B, all binding energy values are less than $-5$ kJ mol$^{-1}$, indicating that the ligand molecules possess an ideal binding affinity [40].

### 3.2. Non-targeted metabolomics

#### 3.2.1. Sample total ion flow diagram (TIC)

The total ion flow plots of QC samples were compared with the overlapping spectra, and the results showed that the response intensities and retention times of the peaks basically overlapped, indicating that the variation caused by the instrument error was small throughout the experiment. The base peak ion (BPI) chromatogram of the QC samples in positive and negative ion mode is shown in Supplementary Fig. 1.

#### 3.2.2. Multivariate statistical analysis

Firstly, PCA was performed, the PCA scores showed that the QC samples showed great aggregation under positive and negative ion modes (Fig. 3D1-D2), indicating that the chromatographic separation and the mass spectrometry collection of the biological samples were relatively stable during the whole analysis process, the accuracy and reliability of the data were well. Furthermore, in the OPLS-DA model (Fig. 3E1-E2), R2 and Q2 meet the requirements. The permutation test results were good, indicating that the model is stable and reliable, and can be used for further data analysis.

#### 3.2.3. Differential metabolites and metabolic pathways

The criterion of fold change (FC) $> 2$ was implied to screen the different metabolites. The metabolites of 6 patients with NAFLD before and after the medication are shown in Tables S4 and S5. All differential metabolites are divided into two categories, including up-regulation and down-regulation. Among them, Quercetin and kaempferol were significantly upregulated differential metabolites. The differential metabolites were submitted to metaboanalyst (version 4.0) for the correlation pathway enrichment analysis to understand the metabolic pathways that were significantly altered. The enrichment analysis results (Fig. 3C) showed the top 50 pathways, the horizontal axis represents enrichment multiple, and the vertical axis represents different metabolic pathways. The size and color depth of the targets were adjusted according to the $P$ value. Among them, thyroid hormone synthesis, androgen and estrogen metabolism, retinol metabolism and sphingolipid metabolism are crucial pathways.

### 3.3. Cellular experimental validation

#### 3.3.1. Effects of quercetin and atorvastatin on HepG2 cell viability and apoptosis

As shown in Fig. 4A and B, CCK-8 results showed that the highest cell viability was observed in the 20 μmol/L quercetin and

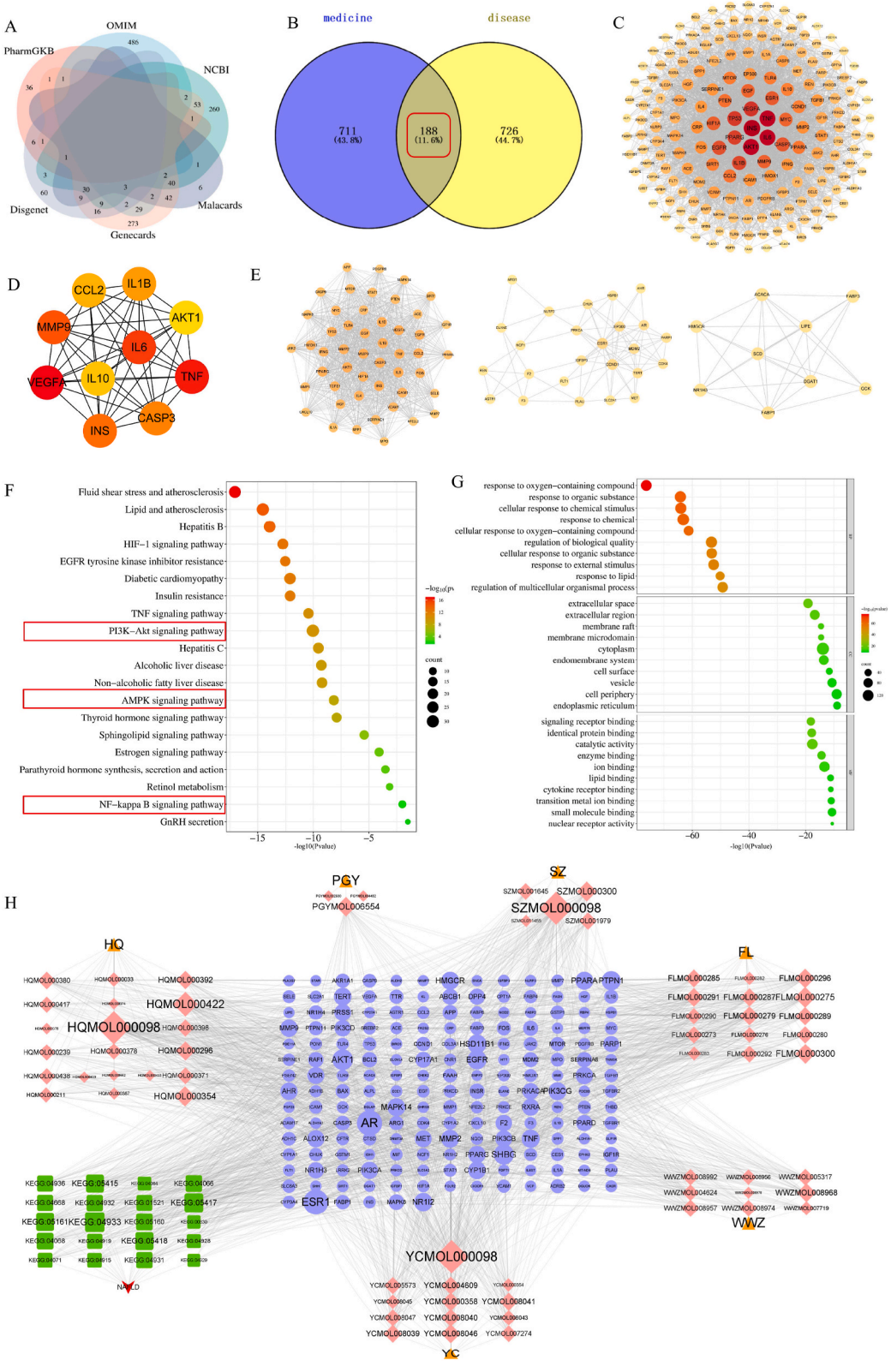


*(caption on next page)*

**Fig. 2.** Network pharmacology analysis results. (A)Targets of NAFLD (B) Venn diagram of the 188 common targets between the active compounds' targets of Shugan Yipi Granule and the disease targets of NAFLD. (C) protein-protein interaction (PPI) network of Shugan Yipi Granule treating NAFLD. (D) Hub genes of Shugan Yipi Granule treating NAFLD. (E) Cluster analysis of the key targets. (F) GO analysis of candidate targets. GO enrichment analysis in metascape showed ten remarkably enriched items in BP, CC, and MF. (G) Significantly enriched information about the top 20 pathways of Shugan Yipi Granule in the treatment of NAFLD. (H) D-C-T-P-D network.

kaempferol group compared to the 0 μmol/L group ($P < 0.05$); And the highest cell viability was observed in the 50 μmol/L atorvastatin group compared to the 0 μmol/L atorvastatin group ($P < 0.05$), shown in Fig. 4C. Therefore, 10 μmol/L, 20 μmol/L and 40 μmol/L concentrations of quercetin, kaempferol and 50 μmol/L atorvastatin for subsequent experiments.

### *3.3.2. Oil red O staining results*

As shown in Fig. 5A and D, in the normal group, the cells were round or oval, with a few lipid droplets between the cells and clear cell boundaries. In the model group, the cells were stained with orange-red color with the microscope, only a single cell had a clear outline, a large number of lipid droplets were formed inside the cell, and the nuclei of some cells were biased to one side of the cell. Orange-red staining was still visible in most of the cells in the experimental and positive control groups, but there were fewer orange-red lipid droplets and smaller lipid droplets compared with the model group, with the least number of red lipid droplets in the post-treatment of quercetin and kaempferol at 40 μmol/$L^{-1}$. The amount of lipid droplets in each group is shown in Fig. 5B and E.This result suggests that quercetin and kaempferol can ameliorate FFA-induced hepatocyte steatosis.

### *3.3.3. Effect of quercetin and kaempferol on TG content in a HepG2 cell*

Compared with the normal group, the TG levels in the model group were significantly higher, and the differences were statistically significant. Compared with the model group, the TG content of both the control and experimental groups was significantly reduced, and the differences were statistically significant, with the lowest TG content in the cells treated with quercetin and kaempferol at a high dose with 40 μmol/$L^{-1}$, as shown in Fig. 5C and F. These results shows that quercetin and kaempferol can reduce FFA-induced lipid accumulation in hepatocytes.

### *3.3.4. Effect of quercetin and kaempferol on free fatty acid uptake in HepG2 cell*

Fig. 6A showed that compared with the normal group, the fatty acid uptake capacity of HepG2 cells in model group was significantly enhanced, compared with the model group, atorvastatin and quercetin significantly inhibited the fatty acid uptake capacity of HepG2 cells. Additionally, compared with medium and low dose groups, high dose (40μmol/L) quercetin had a stronger inhibitory effect on fatty acid uptake capacity of HepG2 cells. Fig. 6B and C showed the fluorescence intensity of HepG2 cells treated with quercetin and kaempferol at a different doses. These results suggest that quercetin and kaempferol may reduce fatty acid-induced lipid accumulation in hepatocytes by inhibiting fatty acid uptake.

## 4. Discussion

NAFLD is a chronic liver disease marked by the accumulation of fat in the liver [48]. It has been reported that Shugan Yipi Granule have the potential to treat NAFLD, as its ingredients can improve steatosis, inflammation and fibrosis in rats caused by a high fat diet [49,50]. Shugan Yipi Granule exert excellent therapeutic effects in protecting the liver, lowering enzymes, alleviating liver inflammation, and improving clinical symptoms [51]. However, the mechanism of Shugan Yipi Granule in the treatment of NAFLD remains unclear. Therefore, network pharmacology, non-targeted metabolomics and in vitro experiment were implied to investigate the potential mechanism of Shugan Yipi Grranule in treating NAFLD. To comprehensively analyze main active compounds and key targets of anti-NAFLD of Shugan Yipi Granule, we used as many online databases as possible to screen drug components and disease targets.

Quercetin, kaempferol and isorhamnetin are crucial active components predicted by network pharmacology. In addition, quercetin and kaempferol are also detected by non-targeted metabolomics in clinical serum samples (Tables S4 and S5). Quercetin have anti-inflammatory, antioxidant, and improving lipid accumulation effects on the liver of ob/ob mice. Its mechanism may be affecting the expression of inflammatory cytokines IL6 and IL1B by acting on AGE-RAGE signaling pathway, and improve liver inflammation in ob/ob mice [52]. Kaempferol can alleviate lipid accumulation and oxidative stress induced by oil acid (OA) in human hepatocellular carcinomas 2 (HepG2) cells. Its mechanism may be direct bind to stearoyl-CoA desaturase 1(SCD-1) to inhibit the expression of lipogenic protein(SREBP1, FAS and SCD-1), lipid droplet protein(Perilipin-1 and Caveolin-1), and finally reduce lipid accumulation and oxidative stress in HepG2 cells induced by oleic acid (OA) [53]. Isorhamnetin can improve steatosis of liver. Its mechanism may be that isorhamnetin acts as a PPAR- γ antagonists may improve liver steatosis by activating mitochondrial respiratory chain (MRC) activity in obese mice [54].

As described in Fig. 5, INS, IL6, AKT1 and other 7 genes are the hub gene of Shugan Yipi Granule in treating NAFLD. And the docking results showed that the binding energies of AKT1, INS, IL6 and other core targets with key compounds were all less than −5 kJ/mol, indicating that they could bind stably. INS comes from humans and vertebrates and encodes the hormone insulin, which is a key regulator of metabolism [55]. Impaired INS function, known as insulin resistance, is a key factor in inducing NAFLD [56]. AKT1 is a subtype of AKT that involves important processes such as cell growth and division, apoptosis inhibition, and adipocyte metabolism. Decreased mRNA levels lead to inhibition of the AKT-mTOR-S6K signaling pathway in liver cells, thereby affecting the development of non-alcoholic fatty liver disease [57]. IL6 can be produced by T cells, B cells, macrophages and endothelial cells, which is a cytokine

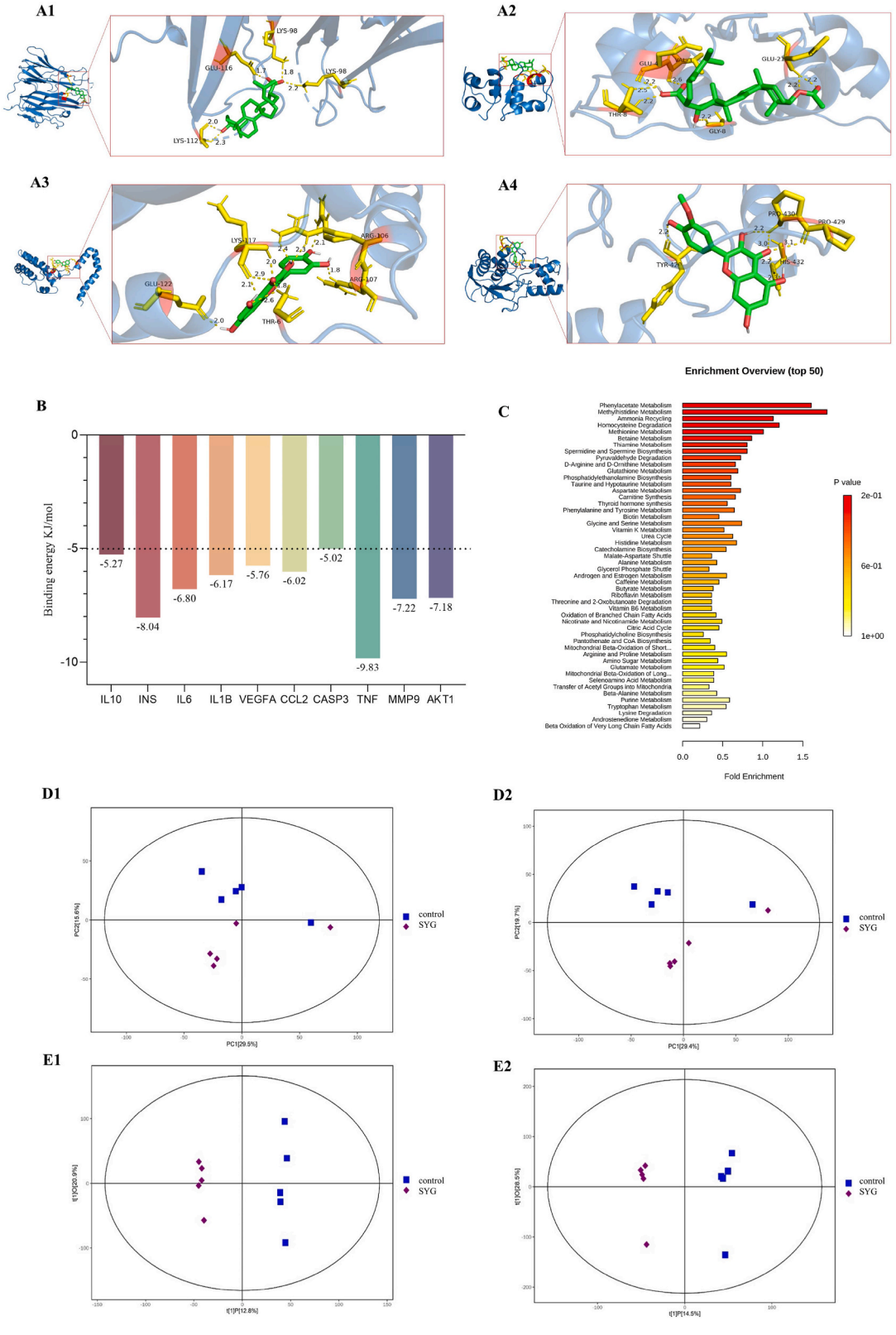


*(caption on next page)*

**Fig. 3.** The molecular docking and non-target metabolomics results. (A1) Represents Pachymic acid and INS docking (A2) Represents Quercetin and IL10 docking (A3) Represents Trametenolic acid and TNF docking. (A4) Represents Isorhamnetin and MMP9 docking; (B) Detailed binding energy information. (C) Enrichment analysis. (D1-D2) PCA diagrams in positive and negative ion modes respectively. (E1-E2) O-PLSDA diagrams in positive and negative ion modes respectively.

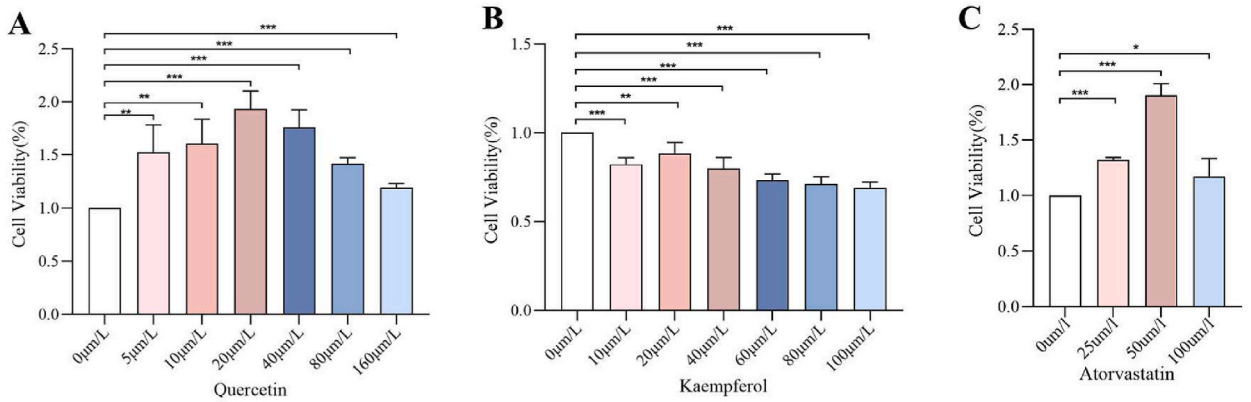


**Fig. 4.** HepG2 cell viability and apoptosis. (A) Effect of quercetin on HepG2 Hepatocyte Activity by Different Concentrations of Quercetin(n = 3). (B) Effect of kaempferol on HepG2 Hepatocyte Activity by Different Concentrations of Quercetin(n = 3) (C) Effect of atorvastatin on the activity of HepG2 hepatocytes(n = 3). Data are expressed as mean ± SD; ***$p < 0.001$, **$p < 0.01$, *$p < 0.05$.

with multiple physiological effects and an important inflammatory factor. IL6 can protect the liver from damage by inhibiting oxidative stress and regulating mitochondrial dysfunction, thereby regulating the occurrence and development of NAFLD [58].

Significant enrichment of NAFLD-related pathways included the PI3K-AKT signaling pathway, AMPK signaling pathway and NF-kappa B signaling pathway. The PI3K/AKT signaling pathway is the main pathway for insulin information transmission, plays an important role in various cellular biological processes such as cell proliferation, differentiation, apoptosis, protein formation, and metabolism [59]. PI3K/AKT signaling pathway disorders can lead to a decrease in insulin sensitivity in the body, also known as insulin resistance (IR), thereby promoting the occurrence and development of NAFLD [60]. AMPK signaling pathway is known as the "receptor of cellular energy balance" and is one of the key pathways leading to the occurrence and development of NAFLD [61]. The activation of AMPK signaling pathway can further inhibit the expression of SREBP-1c and FASN, improving liver lipid metabolism. NF-kappa B signaling pathway is closely related to oxidative stress, inflammation and apoptosis of liver cells in liver tissues. The inhibition of NF-kappa B signaling pathway can further reduce the secretion of TNF-α, IL6 and other pro-inflammatory factors in the liver, thereby reducing the typical inflammatory reaction of NAFLD, and ultimately delaying the progression of NAFLD [62].

According to the integrating analysis of KEGG pathways and metabolic pathways, thyroid hormone synthesis and androgen and estrogen metabolism are the common pathways. Thyroid hormone is a key hormone secreted by thyroid gland to regulate human metabolism, development and growth. The liver is not only the main place for thyroid hormone metabolism, but also the main place for tetraiodothyronine (T4) deiodination to transform into triiodothyronine (T3), and also the main organ for synthesis of thyroid hormone binding globulin and thyroid hormone pre binding protein [63]. It is well known that oxidative stress plays an important role in the progression of NAFLD, type 2 diabetes and other metabolic diseases [64]. T3 may play an anti-oxidative and anti-apoptotic role by activating PI3K/AKT signaling pathway [65]. Therefore, the imbalance of thyroid hormone metabolism and secretion caused by thyroid dysfunction have impact on the progress of NAFLD. Both estrogen and androgen are steroid sex hormones, in addition to their roles in the reproductive system, the imbalance of estrogen and androgen metabolism also directly or indirectly affects lipid metabolism and insulin sensitivity, and ultimately affects the progression of NAFLD [66]. Estrogen cholestasis induces liver inflammation, both gut and liver oxidative stress and apoptosis, involving in activating PI3K/Akt and MAPK signaling pathways [67]. Liver is the main target organ of sex hormone metabolism, liver disease will interfere with the level of sex hormones in the body, at the same time, sex hormones also affect or change the physiological function of liver disease through a variety of mechanisms [68]. Therefore, maintaining the normal secretion and metabolism of sex hormones is of positive significance for the prevention and treatment of non-alcoholic fatty liver [69].

Interestingly, our study showed that quercetin and kaempferol, the main active ingredient of Shugan Yipi Granule, significantly reduced lipid deposition and TG levels in NAFLD cell models, with the most significant effect of quercetin and kaempferol at a concentration of 40 μmol/$L^{-1}$. The free fatty uptake of the cell was inhibited with the increasing concentrations of quercetin and kaempferol, which means quercetin and kaempferol may reduce lipid accumulation in hepatocytes by inhibiting fatty acid uptake.

There are several limitations that need to be addressed in our future study. Firstly, some related pathways of Shugan Yipi Granule have not been experimentally verified. Therefore, we need to establish animal models for validation in future research. The screening of active ingredients is based on databases and previously published literature, so the pharmacological research of Shugan Yipi Granule needs to be included.

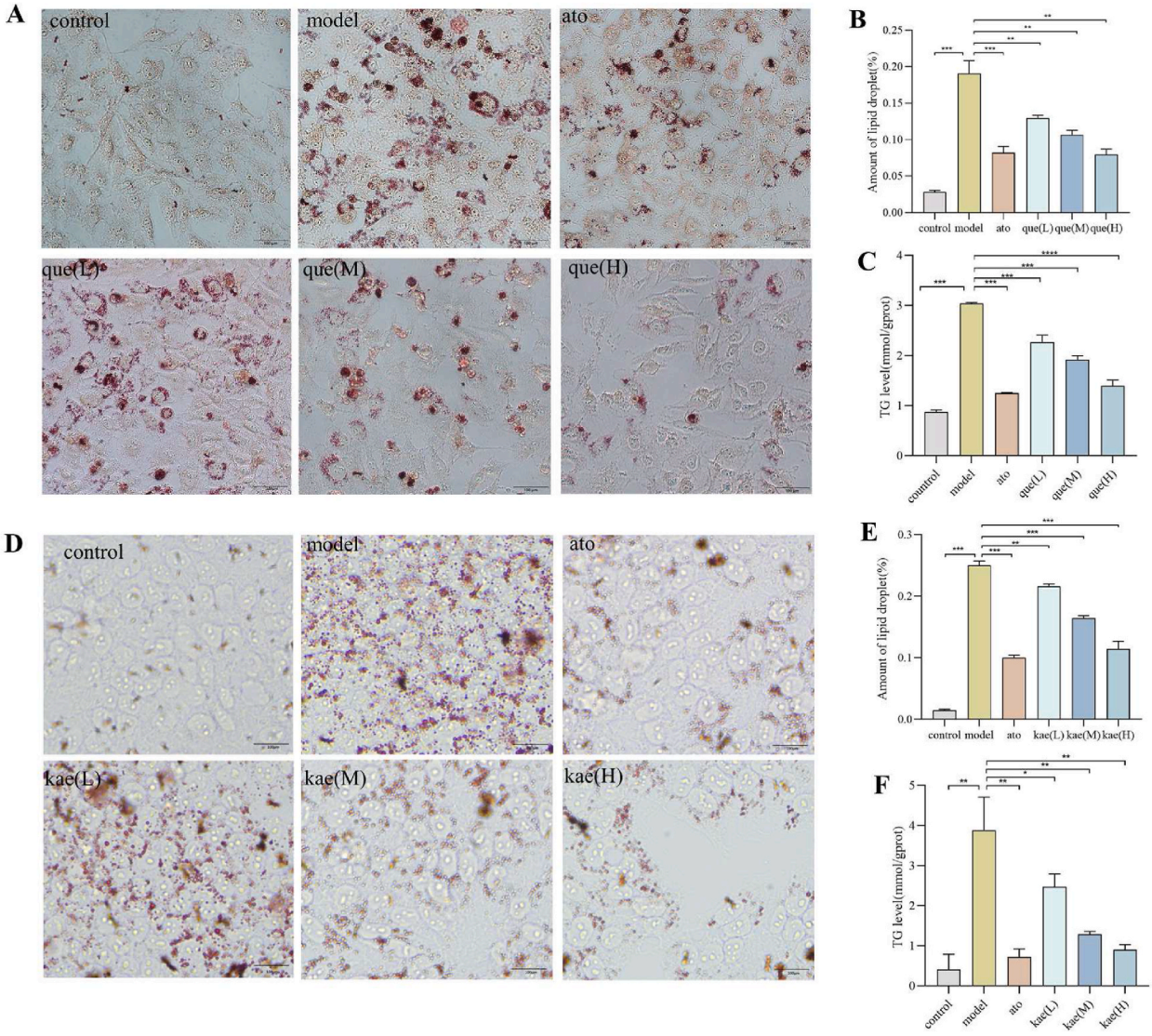


**Fig. 5.** The oil red O staining and TG content of the HepG2 cell. (A) The results of oil red O staining of quercetin on HepG2 cell(n = 3). (B) Quercetin on HepG2 cell's number of lipid droplets in oil red O staining (n = 3). (C) Effect of quercetin on the TG content in HepG2 cells (n = 3). (D) The results of oil red O staining of kaempferol on HepG2 cell(n = 3). (E) Kaempferol on HepG2 cell's number of lipid droplets in oil red O staining (n = 3). (F) Effect of kaempferol on the TG content in HepG2 cells (n = 3). Data are expressed as mean ± SD; $^{****}p < 0.0001$, $^{***}p < 0.001$, $^{**}p < 0.01$, $^{*}p < 0.05$.

## 5. Conclusion

In current research, we used network pharmacology and molecular docking to preliminarily predict the main active ingredient like quercetin, kaempferol and potential targets like INS, AKT1 of Shugan Yipi Granule act on NAFLD. Non-targeted metabolomics revealed that quercetin and kaempferol were significantly up-regulated differential metabolites, which we infer they may involve in KEGG pathways including the PI3K/AKT signaling pathway, AMPK singling pathway, and NF-Kappa B signaling pathway. Further in vitro experiments demonstrated that quercetin and kaempferol, the main active ingredient of Shugan Yipi Granule, attenuated the lipid deposition and TG content of FFA-induced HepG2 cell by inhibiting the fatty acid uptake. It provides the necessary experimental support for future in-depth mechanizes studies.

## Funding

This study was supported by grants from Science and Technology Program of Guangzhou (20221330130037), National Nature Science Foundation of China (82104716) and Guangdong Province Graduate Education Innovation Program Project (2022SFKC073).

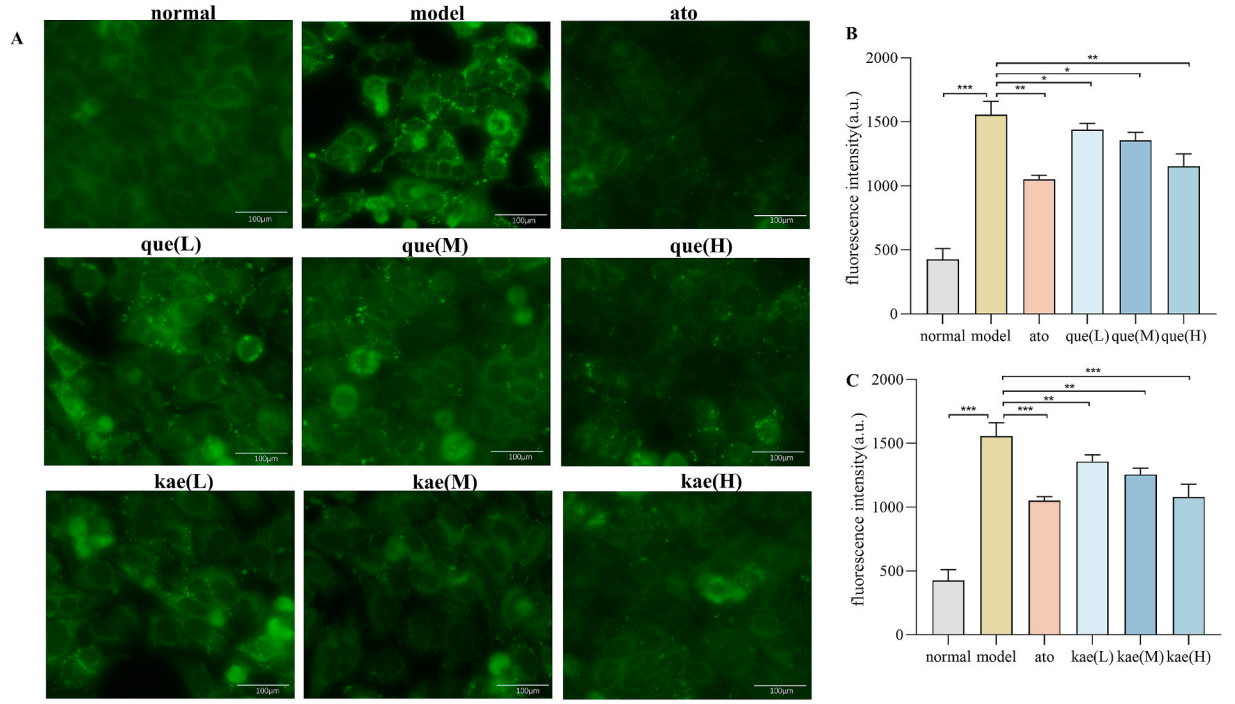


**Fig. 6.** The free fatty acid uptake in HepG2 cell. (A) The images of the fatty acid uptake probe (n = 3). (B) Fluorescence intensity in different doses group of quercetin (n = 3). (C) Fluorescence intensity in different doses group of kaempferol (n = 3). Data are expressed as mean ± SD; ***$p < 0.001$, **$p < 0.01$, *$p < 0.05$.

## CRediT authorship contribution statement

**Hairong Li:** Writing – original draft. **lijun Niu:** Supervision, Writing – review & editing. **Meiling Wang:** Data curation, Visualization. **Chunmei Liu:** Software, Visualization. **Yunlong Wang:** Data curation, Visualization. **Yu Su:** Data curation, Visualization. **Yubin Yang:** Funding acquisition, Supervision, Writing – review & editing.

## Declaration of competing interest

The authors declare that they have no known competing financial interests or personal relationships that could have appeared to influence the work reported in this paper.

## Acknowledgments

Shugan Yipi Granule used in current study is provided by Yuanhesheng (Hong Kong) Pharmaceutical Group.

## Appendix A. Supplementary data

Supplementary data to this article can be found online at https://doi.org/10.1016/j.heliyon.2024.e35491.

## References

[1] Z.M. Younossi, et al., Global epidemiology of nonalcoholic fatty liver disease-Meta-analytic assessment of prevalence, incidence, and outcomes, Hepatology 64 (2016) 73–84, https://doi.org/10.1002/hep.28431.
[2] H. Tilg, G. Targher, NAFLD-related mortality: simple hepatic steatosis is not as 'benign' as thought, Gut 70 (2021) 1212–1213, https://doi.org/10.1136/gutjnl-2020-323188.
[3] Z. Younossi, et al., Global burden of NAFLD and NASH: trends, predictions, risk factors and prevention, Nat. Rev. Gastroenterol. Hepatol. 15 (2018) 11–20, https://doi.org/10.1038/nrgastro.2017.109.
[4] X. Dai, et al., Traditional Chinese Medicine in nonalcoholic fatty liver disease: molecular insights and therapeutic perspectives, Chin. Med. 16 (2021) 68, https://doi.org/10.1186/s13020-021-00469-4.
[5] Q. Fan, F. Xu, B. Liang, X. Zou, The anti-obesity effect of traditional Chinese medicine on lipid metabolism, Front. Pharmacol. 12 (2021) 696603, https://doi.org/10.3389/fphar.2021.696603.

[6] T. Yan, et al., Herbal drug discovery for the treatment of nonalcoholic fatty liver disease, Acta Pharm. Sin. B 10 (2020) 3–18, https://doi.org/10.1016/j.apsb.2019.11.017.
[7] L. Youming Qin, zoubin, Clinical observation on the treatment of viral hepatitis with shugan Yipi granules, Journal of practical traditional chinese internal medcine 7 (1) (2007).
[8] F.Z. Li Wu, Shizhong Zheng, Zhipeng Chen, Baokang Cai, Research progress in the treatment of non-alcoholic fatty liver with traditional Chinese medicine, Chin. Tradit. Pat. Med. 5 (2015) 4.
[9] Y.-C. Huang, et al., Astragalus membranaceus-polysaccharides ameliorates obesity, hepatic steatosis, neuroinflammation and cognition impairment without affecting amyloid deposition in metabolically stressed APPswe/PS1dE9 mice, Int. J. Mol. Sci. 18 (2017), https://doi.org/10.3390/ijms18122746.
[10] Y. Li, H. Y, Y.L. Cai, H.Y. Lin, H.X. Liu, Effect of total astragalus flavonoids on liver fibrosis induced by carbon tetrachloride in rats, Chin. Tradit. Pat. Med. 41 (2019) 1710–1713.
[11] C. Li, et al., Vitexin ameliorates chronic stress plub high fat diet-induced nonalcoholic fatty liver disease by inhibiting inflammation, Eur. J. Pharmacol. 882 (2020) 173264, https://doi.org/10.1016/j.ejphar.2020.173264.
[12] M. Davaatseren, et al., Taraxacum official (dandelion) leaf extract alleviates high-fat diet-induced nonalcoholic fatty liver, Food Chem. Toxicol. 58 (2013) 30–36, https://doi.org/10.1016/j.fct.2013.04.023.
[13] A.L. Hopkins, Network pharmacology: the next paradigm in drug discovery, Nat. Chem. Biol. 4 (2008) 682–690, https://doi.org/10.1038/nchembio.118.
[14] M. Wang, et al., Metabolomics highlights pharmacological bioactivity and biochemical mechanism of traditional Chinese medicine, Chem. Biol. Interact. 273 (2017) 133–141, https://doi.org/10.1016/j.cbi.2017.06.011.
[15] J. Ru, et al., TCMSP: a database of systems pharmacology for drug discovery from herbal medicines, J. Cheminf. 6 (2014) 13, https://doi.org/10.1186/1758-2946-6-13.
[16] Z. Liu, et al., BATMAN-TCM: a bioinformatics analysis tool for molecular mechANism of traditional Chinese medicine, Sci. Rep. 6 (2016) 21146, https://doi.org/10.1038/srep21146.
[17] H.Y. Xu, et al., ETCM: an encyclopaedia of traditional Chinese medicine, Nucleic Acids Res. 47 (2019) D976–D982, https://doi.org/10.1093/nar/gky987.
[18] W. Wu, et al., Systems pharmacology-based strategy to investigate pharmacological mechanisms of radix puerariae for treatment of hypertension, Front. Pharmacol. 11 (2020) 345, https://doi.org/10.3389/fphar.2020.00345.
[19] A. Daina, O. Michielin, V. Zoete, SwissTargetPrediction: updated data and new features for efficient prediction of protein targets of small molecules, Nucleic Acids Res. 47 (2019) W357–W364, https://doi.org/10.1093/nar/gkz382.
[20] M. Safran, et al., GeneCards Version 3: the human gene integrator, Database (2010) baq020, https://doi.org/10.1093/database/baq020, 2010.
[21] J.S. Amberger, C.A. Bocchini, F. Schiettecatte, A.F. Scott, A. Hamosh, OMIM.org: online Mendelian Inheritance in Man (OMIM(R)), an online catalog of human genes and genetic disorders, Nucleic Acids Res. 43 (2015) D789–798, https://doi.org/10.1093/nar/gku1205.
[22] J.M. Barbarino, M. Whirl-Carrillo, R.B. Altman, T.E. Klein, PharmGKB: a worldwide resource for pharmacogenomic information, Wiley Interdiscip Rev Syst Biol Med 10 (2018) e1417, https://doi.org/10.1002/wsbm.1417.
[23] J. Piñero, et al., DisGeNET: a comprehensive platform integrating information on human disease-associated genes and variants, Nucleic Acids Res. 45 (2017) D833–D839, https://doi.org/10.1093/nar/gkw943.
[24] D.S. Wishart, et al., DrugBank 5.0: a major update to the DrugBank database for 2018, Nucleic Acids Res. 46 (2018) D1074–D1082, https://doi.org/10.1093/nar/gkx1037.
[25] T. Barrett, et al., NCBI GEO: archive for functional genomics data sets–update, Nucleic Acids Res. 41 (2013) D991–995, https://doi.org/10.1093/nar/gks1193.
[26] S. Kim, et al., PubChem in 2021: new data content and improved web interfaces, Nucleic Acids Res. 49 (2021) D1388–D1395, https://doi.org/10.1093/nar/gkaa971.
[27] D. Szklarczyk, et al., The STRING database in 2021: customizable protein-protein networks, and functional characterization of user-uploaded gene/measurement sets, Nucleic Acids Res. 49 (2021) D605–D612, https://doi.org/10.1093/nar/gkaa1074.
[28] L. Zhang, et al., Network pharmacology approach to uncover the mechanism governing the effect of radix achyranthis bidentatae on osteoarthritis, BMC Complement Med Ther 20 (2020) 121, https://doi.org/10.1186/s12906-020-02909-4.
[29] P. Shannon, et al., Cytoscape: a software environment for integrated models of biomolecular interaction networks, Genome Res. 13 (2003) 2498–2504, https://doi.org/10.1101/gr.1239303.
[30] H. Ma, Z. He, J. Chen, X. Zhang, P. Song, Identifying of biomarkers associated with gastric cancer based on 11 topological analysis methods of CytoHubba, Sci. Rep. 11 (2021) 1331, https://doi.org/10.1038/s41598-020-79235-9.
[31] C.-H. Chin, et al., cytoHubba: identifying hub objects and sub-networks from complex interactome, BMC Syst. Biol. 8 (2014), https://doi.org/10.1186/1752-0509-8-s4-s11.
[32] U. Raudvere, et al., g:Profiler: a web server for functional enrichment analysis and conversions of gene lists (2019 update), Nucleic Acids Res. 47 (2019) W191–W198, https://doi.org/10.1093/nar/gkz369.
[33] Expansion of the gene ontology knowledgebase and resources, Nucleic Acids Res. 45 (2017) D331–D338, https://doi.org/10.1093/nar/gkw1108.
[34] W. Huang da, B.T. Sherman, R.A. Lempicki, Bioinformatics enrichment tools: paths toward the comprehensive functional analysis of large gene lists, Nucleic Acids Res. 37 (2009) 1–13, https://doi.org/10.1093/nar/gkn923.
[35] J. Wang, et al., Study on the mechanism of Shugan Lidan Xiaoshi granule in preventing acute pancreatitis based on network pharmacology and molecular docking, Heliyon 10 (2024) e27365, https://doi.org/10.1016/j.heliyon.2024.e27365.
[36] S.K. Burley, et al., Protein data bank: a comprehensive review of 3D structure holdings and worldwide utilization by researchers, educators, and students, Biomolecules 12 (2022), https://doi.org/10.3390/biom12101425.
[37] D. Seeliger, B.L. de Groot, Ligand docking and binding site analysis with PyMOL and Autodock/Vina, J. Comput. Aided Mol. Des. 24 (2010) 417–422, https://doi.org/10.1007/s10822-010-9352-6.
[38] M.A. Lill, M.L. Danielson, Computer-aided drug design platform using PyMOL, J. Comput. Aided Mol. Des. 25 (2010) 13–19, https://doi.org/10.1007/s10822-010-9395-8.
[39] S. Forli, et al., Computational protein-ligand docking and virtual drug screening with the AutoDock suite, Nat. Protoc. 11 (2016) 905–919, https://doi.org/10.1038/nprot.2016.051.
[40] C. Li, et al., A systems pharmacology approach for identifying the multiple mechanisms of action for the rougui-fuzi herb pair in the treatment of cardiocerebral vascular diseases, Evid Based Complement Alternat Med (2020) 5196302, https://doi.org/10.1155/2020/5196302, 2020.
[41] M.R. Lee, H.J. Yang, K.I. Park, J.Y. Ma, Lycopus lucidus Turcz. ex Benth. Attenuates free fatty acid-induced steatosis in HepG2 cells and non-alcoholic fatty liver disease in high-fat diet-induced obese mice, Phytomedicine 55 (2019) 14–22, https://doi.org/10.1016/j.phymed.2018.07.008.
[42] Q. Liu, et al., Nano-fat actuated lipometabolic reprogramming of macrophages for intracellular infections in biofilm microenvironment, Adv. Funct. Mater. (2024), https://doi.org/10.1002/adfm.202405852.
[43] M. Zaoui, et al., Breast-associated adipocytes secretome induce fatty acid uptake and invasiveness in breast cancer cells via CD36 independently of body mass index, menopausal status and mammary density, Cancers 11 (2019), https://doi.org/10.3390/cancers11122012.
[44] W. Zhang, et al., C3aR antagonist alleviates C3a induced tubular profibrotic phenotype transition via restoring PPARα/CPT-1α mediated mitochondrial fatty acid oxidation in renin-dependent hypertension, Frontiers in Bioscience-Landmark 28 (2023), https://doi.org/10.31083/j.fbl2810238.
[45] W. Jiao, et al., Integrated network pharmacology and cellular assay for the investigation of an anti-obesity effect of 6-shogaol, Food Chem. 374 (2022) 131755, https://doi.org/10.1016/j.foodchem.2021.131755.
[46] H. Jiang, et al., Protective effects and mechanisms of yinchen linggui zhugan decoction in HFD-induced nonalcoholic fatty liver disease rats based on network pharmacology and experimental verification, Front. Pharmacol. 13 (2022) 908128, https://doi.org/10.3389/fphar.2022.908128.
[47] X. Li, H. Tang, Q. Tang, W. Chen, Decoding the mechanism of huanglian jiedu decoction in treating pneumonia based on network pharmacology and molecular docking, Front. Cell Dev. Biol. 9 (2021) 638366, https://doi.org/10.3389/fcell.2021.638366.

[48] M. Gong, et al., Mechanism by which Eucommia ulmoides leaves Regulate Nonalcoholic fatty liver disease based on system pharmacology, J. Ethnopharmacol. 282 (2022) 114603, https://doi.org/10.1016/j.jep.2021.114603.
[49] B. Liu, et al., Scoparone improves hepatic inflammation and autophagy in mice with nonalcoholic steatohepatitis by regulating the ROS/P38/Nrf2 axis and PI3K/AKT/mTOR pathway in macrophages, Biomed. Pharmacother. 125 (2020) 109895, https://doi.org/10.1016/j.biopha.2020.109895.
[50] A. Nie, et al., Phytochemistry and pharmacological activities of wolfiporia cocos (F.A. Wolf) ryvarden & gilb, Front. Pharmacol. 11 (2020) 505249, https://doi.org/10.3389/fphar.2020.505249.
[51] C.Y.Z. Yu—xiong, Shugan Yipi keli treatment of 70 cases of chronic hepatitis B, Journal of practical traditional chinese internal medcine 9 (2009) 45–46.
[52] H. Yang, et al., Quercetin improves nonalcoholic fatty liver by ameliorating inflammation, oxidative stress, and lipid metabolism in db/db mice, Phytother Res. 33 (2019) 3140–3152, https://doi.org/10.1002/ptr.6486.
[53] F. Tie, et al., Kaempferol and kaempferide attenuate oleic acid-induced lipid accumulation and oxidative stress in HepG2 cells, Int. J. Mol. Sci. 22 (2021), https://doi.org/10.3390/ijms22168847.
[54] Y. Zhang, et al., Dietary component isorhamnetin is a PPARgamma antagonist and ameliorates metabolic disorders induced by diet or leptin deficiency, Sci. Rep. 6 (2016) 19288, https://doi.org/10.1038/srep19288.
[55] F. Xu, et al., Effects of hydroxy-alpha-sanshool on intestinal metabolism in insulin-resistant mice, Foods 11 (2022), https://doi.org/10.3390/foods11142040.
[56] X. Liu, et al., Insulin induces insulin receptor degradation in the liver through EphB4, Nat. Metab. 4 (2022) 1202–1213, https://doi.org/10.1038/s42255-022-00634-5.
[57] C.H. Li, et al., Berberine induces miR-373 expression in hepatocytes to inactivate hepatic steatosis associated AKT-S6 kinase pathway, Eur. J. Pharmacol. 825 (2018) 107–118, https://doi.org/10.1016/j.ejphar.2018.02.035.
[58] C. Lan, Tumor necrosis factor in patients with different degrees of non alcoholic fatty liver disease- α、 detection and significance of interleukin-6, Modern Digestion & Interventio 21 (2016) 85, https://doi.org/10.3969/j.issn.1672-2159.2016.01.029.
[59] S. Matsuda, M. Kobayashi, Y. Kitagishi, Roles for PI3K/AKT/PTEN pathway in cell signaling of nonalcoholic fatty liver disease, ISRN Endocrinol (2013) 472432, https://doi.org/10.1155/2013/472432, 2013.
[60] L.J. Wang Ning, C.H.A.N.G. Zhanjie, W.E.I. Hailiang, Y.A.N. Shuguang, H.U.I. Yi, L.I. Qian, Research progress of PI3K/AKt signal pathway in non-alcoholic fatty liver disease caused by insulin resistance, Chin. J. Gastroenterol. Hepatol. 28 (2019) 1308, 10.
[61] W.E.I. Liu-ting, H. Z.b., G.A.O. Song-lin, Research progress of traditional Chinese medicine in treatment of nonalcoholic fatty liver disease based on AMPK signaling pathway, World Latest Medicine Information 20 (2023) 12, https://doi.org/10.3969/j.issn.1671-3141.2023.020.003.
[62] J.Y. Yang, Z.H. Shi, W. Ma, D.Q. Tao, S. Liu, L. Chen, X.L. Zhou, Effect of Fuzi Lizhong decoction in reducing liver injury of rats with non-alcoholic fatty liver via activating AMPK and suppressing NF-㐂p65 pathway, China J. Chin. Mater. Med. 43 (2018) 3176.
[63] W.L. Yulin, H. L. Y. W. L. X. L., Levels and clinical significance of thyroid hormones in non-alcoholic fatty liver disease patients, Chin. J. Gastroenterol. Hepatol. 8 (2011) 3.
[64] M. Apostolopoulou, et al., Specific hepatic sphingolipids relate to insulin resistance, oxidative stress, and inflammation in nonalcoholic steatohepatitis, Diabetes Care 41 (2018) 1235–1243, https://doi.org/10.2337/dc17-1318.
[65] B. Zeng, L. Liu, X. Liao, C. Zhang, H. Ruan, Thyroid hormone protects cardiomyocytes from H2O2-induced oxidative stress via the PI3K-AKT signaling pathway, Exp. Cell Res. 380 (2019) 205–215, https://doi.org/10.1016/j.yexcr.2019.05.003.
[66] J.Y. Yim, J. Kim, D. Kim, A. Ahmed, Serum testosterone and non-alcoholic fatty liver disease in men and women in the US, Liver Int. 38 (2018) 2051–2059, https://doi.org/10.1111/liv.13735.
[67] D. Xiang, et al., Estrogen cholestasis induces gut and liver injury in rats involving in activating PI3K/Akt and MAPK signaling pathways, Life Sci. 276 (2021), https://doi.org/10.1016/j.lfs.2021.119367.
[68] Yanjun Dong, Y. T, Muxu Zhai, Lijuan Liu, Relationship between serum level of sex hormone and insulin resistance, the index of liver enzymes in postmenopausal women with non alcoholic fatty liver, Chin. J. Clin. 8 (2014) 2275, https://doi.org/10.3877/cma.j.issn.1674-0785.2014.12.020.
[69] A. Lonardo, A. Mantovani, S. Lugari, G. Targher, NAFLD in some common endocrine diseases: prevalence, pathophysiology, and principles of diagnosis and management, Int. J. Mol. Sci. 20 (2019), https://doi.org/10.3390/ijms20112841.